Supporting Information

New Theoretical Insights into the Crystal-Field Splitting and Transition Mechanism for Nd^{3+} Doped $Y_3Al_5O_{12}$

Meng Ju[1], Yang Xiao[2,3], MingMin Zhong[1], Weiguo Sun[3], Xinxin Xia[3], Yau-yuen Yeung[4,*] and Cheng Lu[2,5,*]

[1]School of Physical Science and Technology, Southwest University, Chongqing 400715, China

[2]Department of Physics, Nanyang Normal University, Nanyang 473061, China

[3]Institute of Atomic and Molecular Physics, Sichuan University, Chengdu 610065, China

[4]Department of Science and Environmental Studies, The Education University of Hong Kong, Tai Po, NT, Hong Kong, China

[5]School of Science, Northwestern Polytechnic University, Xi'an 710072, China

*Correspondence author. E-mail: yyyeung@eduhk.hk (Yau-yuen Yeung) and lucheng@calypso.cn (Cheng Lu)

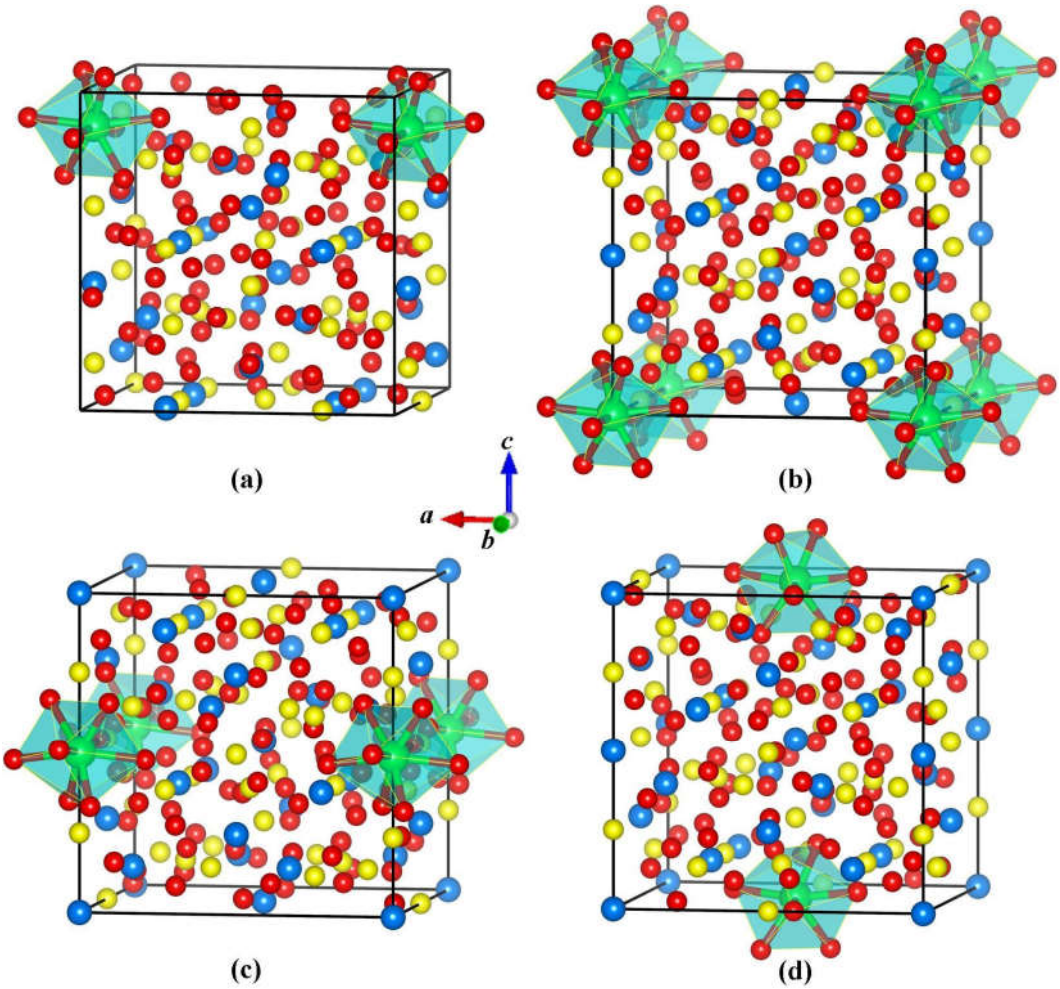

Figure S1. Coordination structures the optimized metastable (a), (b), (c) and (d) for Nd:YAG. The red, yellow, blue and green spheres represent O, Al, Y and Nd atoms, respectively.

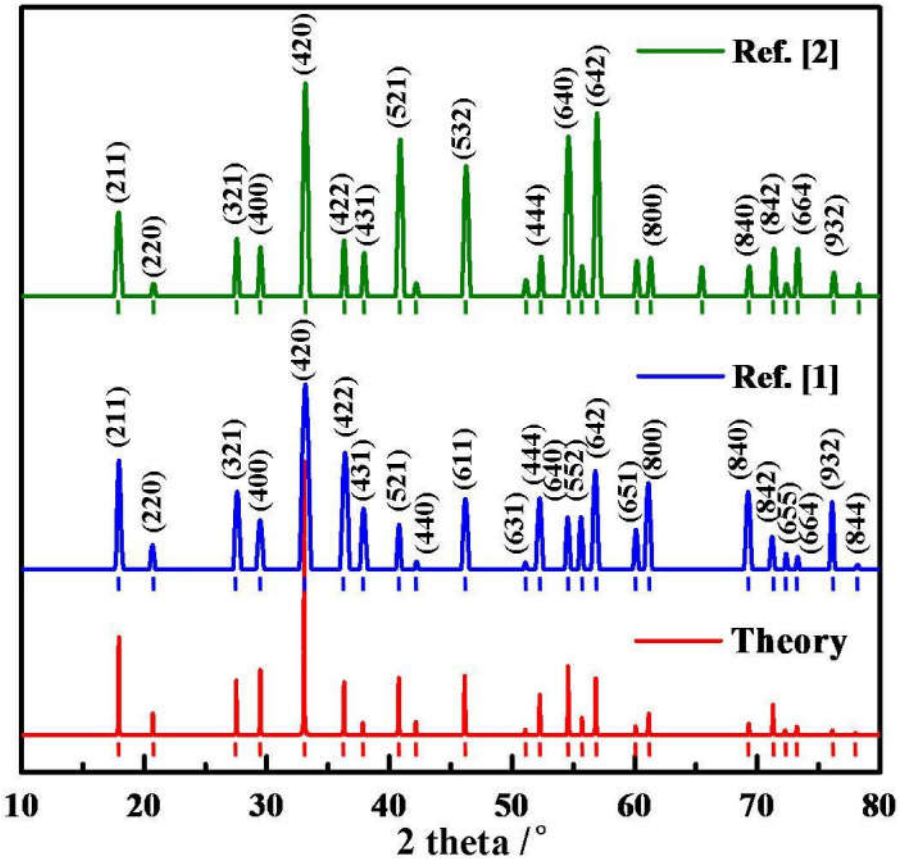

Figure S2. The simulated complete XRD patterns of Nd:YAG compared with experimental data.

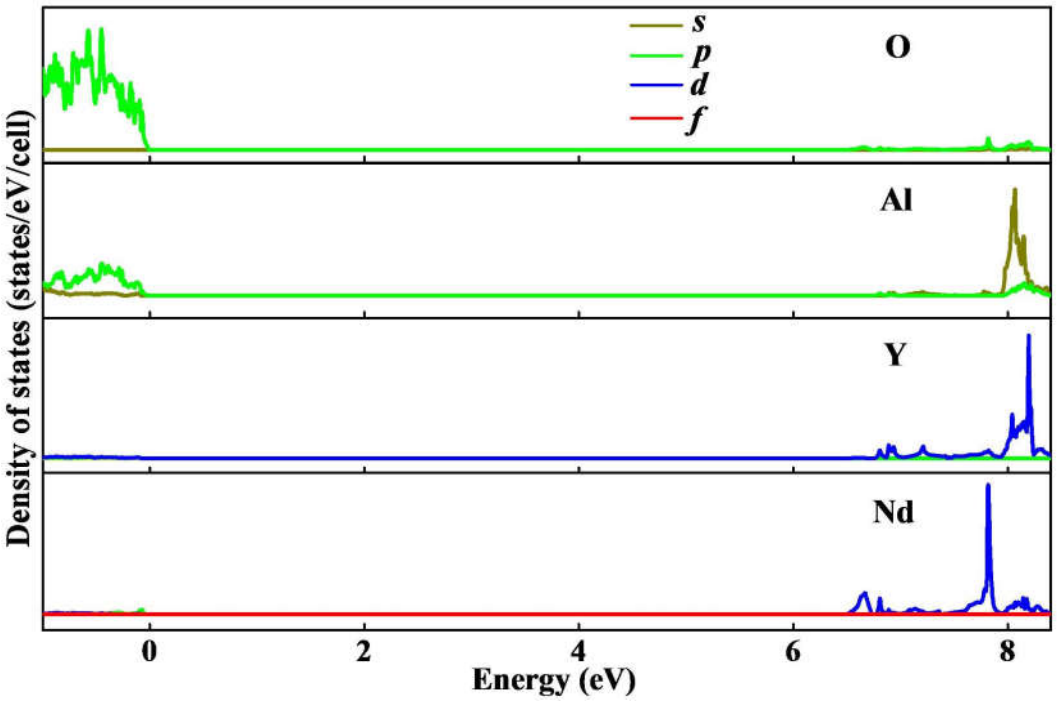

Figure S3. The calculated partial density of states for Nd:YAG.

Table S1. Lattice constants *a*, *b* and *c*, unit-cell volume, relative energies for the ground state and metastable Nd:YAG crystals.

	Space group	*a* (Å)	*b* (Å)	*c* (Å)	*V* (Å^3)	ΔE ($\times 10^{-2}$ meV)
Nd:YAG	C_{222}	12.1145	12.1145	12.1145	1777.94	0
Isomer (a)	P_1	12.1146	12.1146	12.1220	1779.07	0.42
Isomer (b)	C_{222}	12.1145	12.1145	12.1222	1779.07	0.47
Isomer (c)	C_{222}	12.1146	12.1146	12.1223	1779.11	1.25
Isomer (d)	P_1	12.1145	12.1145	12.1222	1779.06	18.76

Table S2. The experimental and calculated Stark energy levels (all in cm^{-1}) of Nd^{3+} in YAG.

			Present work		Other[3]					Present work		Other[3]	
$^{2S+1}L_J$	State	E_{obs}[3]	E_{calc}	ΔE	E_{calc}	ΔE	$^{2S+1}L_J$	State	E_{obs}[3]	E_{calc}	ΔE	E_{calc}	ΔE
$^4I_{9/2}$	1	0	−12	−12	−4	−4		87	—	21505	—	21491	—
	2	130	130	0	142	12		88	21522	21524	2	21514	−8
	3	199	197	−2	205	6		89	21593	21612	19	21608	15
	4	308	311	3	328	20		90	21661	21674	13	21664	3
	5	857	850	−7	870	13		91	21697	21700	3	21709	12
$^4I_{11/2}$	6	2002	2004	2	1990	−12		92	21767	21766	−1	21754	−13
	7	2029	2028	−1	2017	−12		93	21791	21781	−10	21782	−9
	8	2110	2109	−1	2102	−8		94	—	21844	—	21851	—
	9	2147	2148	1	2140	−7		95	21872	21863	−9	21866	−6
	10	2468	2465	−3	2465	−3		96	21906	21914	8	21906	0
	11	2521	2523	2	2524	3		97	22036	22063	27	22043	7
$^4I_{13/2}$	12	3922	3928	6	3908	−14	$^2P_{1/2}$	98	23155	23122	−33	23135	−20
	13	3930	3932	2	3916	−14	$^2D(1)_{5/2}$	99	23674	23654	−20	23685	11
	14	4032	4036	4	4026	−6		100	23764	23757	−7	23764	0
	15	4047	4054	7	4041	−6		101	23849	23848	−1	23838	−11
	16	4435	4430	−5	4421	−14	$^2P_{3/2}$	102	25994	26003	9	26026	32
	17	4442	4441	−1	4441	−1		103	—	26078	—	26085	—
	18	4498	4506	8	4504	6	$^4D_{3/2}$	104	27571	27562	−9	27550	−21
$^4I_{15/2}$	19	5758	5757	−1	5756	−2	and	105	27670	27677	7	27683	13
	20	5814	5815	1	5804	−10	$^4D_{5/2}$	106	27809	27819	10	27818	9
	21	5936	5942	6	5939	3		107	28183	28192	9	28182	−1
	22	5970	5966	−4	5971	1		108	28263	28268	5	28272	9
	23	6570	6555	−15	6557	−13	$^4D_{1/2}$	109	28359	28355	−4	28374	15

	24	6583	6585	2	6596	13
	25	6639	6641	2	6659	20
	26	6734	6737	3	6758	24
$^4F_{3/2}$	27	11427	11426	–1	11421	–6
	28	11512	11500	–12	11493	–19
$^4F_{5/2}$	29	12370	12354	–16	12359	–11
and	30	12432	12437	5	12436	4
$^2H(2)_{9/2}$	31	12519	12500	–19	12451	–68
	32	12575	12590	15	12610	35
	33	12607	12640	33	12650	43
	34	12623	12646	23	12693	70
	35	12819	12827	8	12811	–8
	36	12840	12844	4	12856	16
$^4F_{7/2}$	37	13363	13355	–8	13364	1
and	38	13433	13426	–7	13440	7
$^4S_{3/2}$	39	13563	13555	–8	13555	–8
	40	13572	13574	2	13572	0
	41	13596	13591	–5	13596	0
	42	13633	13632	–1	13646	13
$^4F_{9/2}$	43	14626	14634	8	14643	17
	44	14678	14675	–3	14685	7
	45	14793	14788	–5	14779	–14
	46	14819	14825	6	14815	–4
	47	14916	14924	8	14914	–2
$^2H(2)_{11/2}$	48	15838	15836	–2	15898	60
	49	15870	15900	30	15920	50
	50	—	15920	—	15946	—
	51	15957	15943	–14	15956	–1
	52	16103	16079	–24	16037	–66

$^2I_{11/2}$	110	28580	28611	31	28601	21
	111	28800	28822	22	28819	19
	112	28930	28956	26	28957	27
	113	29140	29139	–1	29124	–16
	114	29270	29287	17	29258	–12
	115	29360	29382	22	29366	6
$^2L_{15/2}$,	116	29715	29705	–10	29712	–3
$^4D_{7/2}$,	117	29876	29865	–11	29867	–9
and	118	29880	29881	1	29881	1
$^2I_{13/2}$	119	29920	29905	–15	29917	–3
	120	29953	29953	0	29952	–1
	121	—	30054	—	30048	—
	122	30070	30064	–6	30057	–13
	123	30140	30135	–5	30121	–19
	124	30160	30140	–20	30147	–13
	125	30190	30193	3	30198	8
	126	30230	30234	4	30233	3
	127	30289	30270	–19	30283	–6
	128	30360	30340	–20	30350	–10
	129	30400	30387	–13	30389	–11
	130	30464	30453	–11	30442	–22
	131	30495	30504	9	30495	0
	132	30547	30552	5	30550	3
	133	30611	30602	–9	30593	–18
	134	30620	30620	0	30611	–9
$^2L_{17/2}$	135	—	31237	—	31247	—
	136	—	31406	—	31393	—
	137	31440	31441	1	31459	19
	138	31530	31503	–27	31525	–5

	53	16119	16102	−17	16067	−52
$^4G_{5/2}$	54	16849	16852	3	16848	−1
	55	16992	16979	−13	16978	−14
	56	17047	17057	10	17054	7
$^2G_{7/2}$	57	17241	17226	−15	17220	−21
	58	17268	17275	7	17275	7
	59	17322	17296	−26	17302	−20
	60	17575	17565	−10	17594	19
$^4G_{7/2}$	61	18723	18719	−4	18709	−14
	62	18822	18830	8	18831	9
	63	18843	18855	12	18863	20
	64	18986	18968	−18	18987	1
$^2K_{13/2}$	65	19154	19136	−18	19133	−21
and	66	—	19272	—	19262	—
$^4G_{9/2}$	67	19294	19319	25	19317	23
	68	—	19429	—	19421	—
	69	19470	19452	−18	19448	−22
	70	—	19509	—	19499	—
	71	19543	19547	4	19555	12
	72	19596	19586	−10	19593	−3
	73	19651	19666	15	19660	9
	74	19814	19833	19	19823	9
	75	—	19890	—	19870	—
	76	20048	20045	−3	20026	−22
$^2G(1)_{9/2}$,	77	20730	20716	−14	20719	−11
$^2D(1)_{3/2}$,	78	20773	20781	8	20797	24
$^4G_{11/2}$,	79	20790	20787	−3	20819	29
and	80	20803	20802	−1	20833	30
$^2K_{15/2}$	81	20962	20954	−8	20954	−8

	139	31570	31573	3	31567	−3
	140	31585	31598	13	31583	−2
	141	31665	31652	−13	31667	2
	142	—	31776	—	31795	—
	143	—	31903	—	31885	—
$^2H(1)_{9/2}$	144	32613	32614	1	32621	8
	145	32663	32663	0	32662	0
	146	32745	32725	−20	32730	−15
	147	32802	32805	3	32801	−1
	148	32840	32822	−18	32835	−5
$^2D(2)_{3/2}$	149	32980	32970	10	32966	−14
	150	33045	33051	6	33056	11
$^2D(2)_{5/2}$	151	33693	33724	31	33699	6
and	152	—	33800	—	33783	—
$^2H(1)_{11/2}$	153	33840	33837	−3	33830	−10
	154	34050	34080	30	34071	21
	155	34110	34122	12	34123	13
	156	34210	34179	−31	34170	−40
	157	34260	34255	−5	34256	−4
	158	34290	34327	37	34333	43
	159	—	34457	—	34475	—
$^2F(2)_{5/2}$	160	37789	37763	−26	37799	10
	161	37900	37939	39	37920	20
	162	38065	38051	−14	38043	−22
$^2F(2)_{7/2}$	163	39202	39208	6	39232	30
	164	—	39255	—	39251	—
	165	39330	39316	−14	39312	−18
	166	—	39565	—	39553	—
$^2G(2)_{9/2}$	167	—	47000	—	47000	—

82	—	21020	—	21011	—	168	—	47018	—	47010	—
83	21029	21056	27	21057	28	169	47200	47191	–9	47170	–30
84	21080	21076	–4	21072	–8	170	—	47266	—	47247	—
85	21159	21144	15	21141	–18	171	—	47325	—	47266	—
86	21162	21150	–12	21152	–10						

Table S3. Calculated wavelengths (λ), ED (A_{ED}) and MD (A_{MD}) radiative decay rates, branching ratios (β) and radiative lifetimes (τ) for spontaneous emission transitions between the first 11 excited states in Nd:YAG. Available theoretical and experimental results are also listed for comparison.

Transition		λ (nm)		A_{ED} (s^{-1})	A_{MD} (s^{-1})	A_{total} (s^{-1})		β		τ (μs)	
		Present	Other			Present	Other	Present	Other	Present	Other
$^4I_{11/2}$	$^4I_{9/2}$	5359		13.4	1.6	15.0		1		66541	
$^4I_{13/2}$	$^4I_{9/2}$	2609		37.6	0	37.6		0.69		18429	
	$^4I_{11/2}$	5085		14.4	2.2	16.6		0.31			
$^4I_{15/2}$	$^4I_{9/2}$	1707		11.5	0	11.5		0.18		15795	
	$^4I_{11/2}$	2504		34.2	0	34.2		0.54			
	$^4I_{13/2}$	4933		16.0	1.6	17.6		0.28			
$^4F_{3/2}$	$^4I_{9/2}$	897	885[4], 900[5]	1254.2	0	1254.2	1420[7]	0.34	0.32[7]	274	259±25[7], 250±25[9]
	$^4I_{11/2}$	1077	1073[6]	1962.0	0	1962.0	1940[7]	0.54	0.54[7]		
	$^4I_{13/2}$	1367	1350[7], 1340[4]	415.8	0	415.8	473[7]	0.11	0.14[7]		
	$^4I_{15/2}$	1891	1850[5], 1800[7]	20.9	0	20.9	15[7]	0.01	0.003[7]		
$^4F_{5/2}$	$^4I_{9/2}$	822	809[4], 808[8]	3192.3	0	3192.3		0.66		207	
	$^4I_{11/2}$	970		476.7	0	476.7		0.10			
	$^4I_{13/2}$	1200		976.2	0	976.2		0.20			
	$^4I_{15/2}$	1584		195.3	0	195.3		0.04			
$^2H(2)_{9/2}$	$^4I_{9/2}$	811		488.8	6.9	495.7		0.58		1177	
	$^4I_{11/2}$	955		67.9	4.2	72.1		0.09			

	$^4I_{13/2}$	1176	167.7	0	167.7	0.20	
	$^4I_{15/2}$	1544	113.5	0	113.5	0.13	
$^4F_{7/2}$	$^4I_{9/2}$	762	2572.7	0.1	2572.8	0.50	193
	$^4I_{11/2}$	889	1562.3	0	1562.3	0.30	
	$^4I_{13/2}$	1077	366.2	0	366.2	0.07	
	$^4I_{15/2}$	1378	677.6	0	677.6	0.13	
$^4S_{3/2}$	$^4I_{9/2}$	755	2776.3	0	2776.3	0.43	156
	$^4I_{11/2}$	879	1566.3	0	1566.3	0.24	
	$^4I_{13/2}$	1062	1389.1	0	1389.1	0.22	
	$^4I_{15/2}$	1354	674.4	0	674.4	0.11	
$^4F_{9/2}$	$^4I_{9/2}$	694	264.1	1.9	266.0	0.06	237
	$^4I_{11/2}$	798	1539.3	1.7	1541.0	0.37	
	$^4I_{13/2}$	946	1483.9	0	1483.9	0.35	
	$^4I_{15/2}$	1171	912.9	0	912.9	0.22	
$^2H(2)_{11/2}$	$^4I_{9/2}$	638	79.0	0	79.0	0.28	3592
	$^4I_{11/2}$	725	54.6	2.6	57.2	0.21	
	$^4I_{13/2}$	845	35.7	5.7	41.4	0.15	
	$^4I_{15/2}$	1020	73.0	0	73.0	0.26	
	$^4F_{3/2}$	2215	1.4	0	1.4	0.01	
	$^4F_{5/2}$	2865	2.0	0	2.0	0.01	
	$^2H(2)_{9/2}$	3007	17.6	1.9	19.5	0.07	
	$^4F_{7/2}$	3930	3.9	0	3.9	0.01	
$^4G_{5/2}$	$^4I_{9/2}$	597	4651.8	0	4651.8	0.58	124
	$^4I_{11/2}$	672	2783.4	0	2783.4	0.35	
	$^4I_{13/2}$	775	488.8	0	488.8	0.06	
	$^4I_{15/2}$	919	20.7	0	20.7	0.01	

Table S4. The calculated statevectors of the ground state and the first 11 excited states for Nd^{3+} in YAG.

State $^{2s+1}L_J$	Statevector $\|^{2s+1}L_J\rangle$
$^4I_{9/2}$	$0.984\ \|^4I_{9/2}\rangle - 0.168\ \|^2H(2)_{9/2}\rangle + 0.057\ \|^2H(1)_{9/2}\rangle$
$^4I_{11/2}$	$-0.995\ \|^4I_{11/2}\rangle + 0.096\ \|^2H(2)_{11/2}\rangle - 0.036\ \|^2H(1)_{11/2}\rangle$
$^4I_{13/2}$	$-0.998\ \|^4I_{13/2}\rangle - 0.064\ \|^2K_{13/2}\rangle + 0.024\ \|^2I_{13/2}\rangle$
$^4I_{15/2}$	$-0.993\ \|^4I_{15/2}\rangle - 0.115\ \|^2K_{15/2}\rangle + 0.009\ \|^2L_{15/2}\rangle$
$^4F_{3/2}$	$-0.970\ \|^4F_{3/2}\rangle - 0.224\ \|^2D(1)_{3/2}\rangle + 0.062\ \|^2D(2)_{3/2}\rangle$
$^4F_{5/2}$	$-0.988\ \|^4F_{5/2}\rangle - 0.147\ \|^2D(1)_{5/2}\rangle + 0.033\ \|^2F(2)_{5/2}\rangle$
$^2H(2)_{9/2}$	$-0.731\ \|^2H(2)_{9/2}\rangle + 0.385\ \|^4F_{9/2}\rangle - 0.340\ \|^2G(1)_{9/2}\rangle$
$^4F_{7/2}$	$-0.965\ \|^4F_{7/2}\rangle + 0.199\ \|^2G(1)_{7/2}\rangle - 0.158\ \|^2G(2)_{7/2}\rangle$
$^4S_{3/2}$	$-0.971\ \|^4S_{3/2}\rangle - 0.222\ \|^2P_{3/2}\rangle - 0.073\ \|^4F_{3/2}\rangle$
$^4F_{9/2}$	$0.862\ \|^4F_{9/2}\rangle + 0.454\ \|^2H(2)_{9/2}\rangle - 0.156\ \|^2H(1)_{9/2}\rangle$
$^2H(2)_{11/2}$	$0.894\ \|^2H(2)_{11/2}\rangle - 0.354\ \|^2H(1)_{11/2}\rangle - 0.251\ \|^4G_{11/2}\rangle$
$^4G_{5/2}$	$-0.993\ \|^4G_{5/2}\rangle - 0.083\ \|^2F(1)_{5/2}\rangle - 0.082\ \|^2F(2)_{5/2}\rangle$

Appendix – Method and equations for the calculations of transition intensities

The model Hamiltonian for Nd^{3+} is defined as[10]-[11]

$$H_f = E_{AVE} + \sum_{k=2,4,6} F^k f_k + \zeta_{4f} \times \sum_i \vec{l}_i \cdot \vec{s}_i + \alpha L(L+1) + \beta G(G_2) + \gamma G(R_7) + \sum_{i=2,3,4,6,7,8} T^i t_i + \sum_{j=0,2,4} M^j m_j + \sum_{k=2,4,6} P^k p_k \quad \text{(A1)}$$

where E_{AVE} represents the barycenter energy of the $4f^3$ configuration. The next seven terms represent the Coulomb repulsion, spin-orbit, two-body, three-body, spin-other-orbit and electrostatically correlated spin-orbit interactions. Moreover, F^k and ζ_{4f} are the radial parts of the electrostatic and spin-orbit coupling constant. Two-body and Judd's three-body parameters are represented by α, β, γ and T^i. $G(G2)$ and $G(R7)$ represent the eigenvalues of the Casimir's operators for the Lie groups G_2 and R_7. The remaining parameters, M^j and P^k, are used to represent the Marvin integrals and spin-orbit perturbations.

The crystal field interaction H_{CF} for Nd^{3+} in YAG, in the form of Wybourne normalization, can be expressed as[12]

$$H_{CF} = B_2^0 C_2^0 + B_2^2 (C_2^2 + C_2^{-2}) + B_4^0 C_4^0 + B_4^2 (C_4^2 + C_4^{-2}) + B_4^4 (C_4^4 + C_4^{-4}) + B_6^0 C_6^0 + B_6^2 (C_6^2 + C_6^{-2}) + B_6^4 (C_6^4 + C_6^{-4}) + B_6^6 (C_6^6 + C_6^{-6}) \quad \text{(A2)}$$

where C_q^k are the normalized spherical-tensor operators and B_q^k are the crystal field parameters (CFPs). The values of these CFPs can be determined by the least-squares fit to the observed energy levels.[12]

The ED (A_{ED}) radiative decay rates can be written as[13]-[14]

$$A_{ED(SLJ\to S'L'J')} = \frac{16\pi^3 e^2}{3\varepsilon_0 hc^3}\frac{\nu^3}{(2J+1)}\chi_{ED}\sum_{\lambda=2,4,6}\Omega_{(\lambda)}\left|\left\langle l^N SLJ\left\|U^{(\lambda)}\right\|l^N S'L'J'\right\rangle\right|^2 \tag{A3}$$

where ν is the transition frequency, n is the refractive index and χ_{ED} is the local-field correction for ED induced transitions with the form of $(n^2+1)^2/(9n)$ and $n(n^2+1)^2/9$ for absorption and emission transition, respectively. The Judd-Ofelt intensity parameters $\Omega_{(\lambda)}$ should be summed over λ=2,4,6 for a product with the even-rank reduced matrix elements of the $U^{(\lambda)}$ tensor operator.

The MD (A_{MD}) radiative decay rates can be written as[13]-[14]

$$A_{MD} = \frac{\pi h e^2}{3\varepsilon_0 c^5 m_e^2}\frac{\nu^3}{g}\chi_{MD}\left|\left\langle l^N\psi\left\|L+g_e S\right\|l^N\psi'\right\rangle\right|^2 \tag{A4}$$

where g_e = 2.00232 is the gyromagnetic ratio of the electron and g is the degeneracy of the initial level. χ_{MD} is the local-field correction for MD induced transitions with the form of n and n^3 for the absorption and emission transition, respectively. ψ and ψ' are the statevectors for the initial and terminating levels for the $\psi \to \psi'$ transition, respectively. For transitions between J-multiplets, the statevector takes the form of $\psi(SLJ)$ with $g = (2J+1)$ while for transitions between crystal field levels, it takes the form of $\psi(SLJ\Gamma_i)$.

The radiative lifetime can be written as[13]-[14]

$$\tau_{SLJ} = \frac{1}{\sum_{S'L'J'}(A_{ED(SLJ\to S'L'J')} + A_{MD(SLJ\to S'L'J')})} \tag{A5}$$

The branching ratio can be written as[13]-[14]

$$\beta_{(SLJ \to S'L'J')} = \tau_{SLJ} \times [A_{ED(SLJ \to S'L'J')} + A_{MD(SLJ \to S'L'J')}] \tag{A6}$$

The MD absorption oscillator strengths can be written as[13]-[14]

$$P_{MD} = \frac{h\nu}{6m_e c^2} \frac{n}{(2J+1)} \left| \left\langle l^N SLJ \left\| L + g_e S \right\| l^N SLJ' \right\rangle \right|^2 \tag{A7}$$

Coordinates of all atoms for the ground state Nd:YAG

Atom	*x*	*y*	*z*
Nd	0.50000	0.50000	0.50000
Y1	0.12479	0.24980	-0.12460
Y2	0.37452	0.24891	-0.62590
Y9	0.00000	0.00000	0.00000
Y10	0.00000	-0.50000	-0.24970
Y12	0.87504	0.25006	-0.62507
Y13	0.37494	-0.24993	-0.12472
Y20	0.00000	-0.50000	-0.75044
Y22	-0.00000	-0.00000	-0.50000
Y23	0.50000	-0.50000	-0.00000
Al1	-0.00008	0.24983	0.12499
Al2	0.50048	-0.24854	-0.37389
Al5	0.00013	-0.24976	-0.37489
Al6	0.49981	0.24969	0.12438
Al17	0.37480	0.24966	-0.12514
Al18	0.12480	0.24963	-0.62515
Al21	0.24996	-0.12498	0.12486
Al23	0.24890	-0.37497	-0.37449
Al25	0.00000	-0.00000	-0.24993
Al26	0.00000	-0.50000	0.00014
Al27	0.50000	-0.00000	-0.49984
Al28	0.50000	-0.50000	-0.75245
O1	0.96966	0.19943	-0.02409
O2	0.47044	-0.29614	-0.52395
O5	0.03024	-0.30032	-0.22569
O6	0.53015	0.19951	-0.72657
O9	0.14896	-0.72004	0.07461

O10	0.64961	-0.21972	-0.42473
O11	0.64957	-0.27943	-0.82532
O12	0.14872	0.21957	-0.32453
O17	0.05031	0.10071	-0.84490
O18	0.55170	-0.39698	-0.33916
O19	0.94980	-0.39918	-0.40513
O20	0.44963	0.10066	0.09463
O49	0.03008	-0.70014	-0.72598
O50	0.53005	-0.19820	-0.22522
O53	0.96986	-0.19956	-0.52415
O54	0.46963	-0.69995	-0.02458
O57	0.85068	0.21985	-0.82461
O58	0.35080	-0.28069	-0.32493
O59	0.35077	-0.21964	0.07426
O60	0.85114	-0.72018	-0.42514
O65	0.94982	-0.60105	0.09467
O66	0.44932	-0.10020	-0.40455
O67	0.05040	-0.10069	-0.34477
O68	0.55039	-0.60136	-0.84615

References

[1] Kostić, S.; Lazarević, Z.; Radojević, V.; Milutinović, A.; Romčević, M.; Romčević, N. Z.; Valčić, A. Study of Structural and Optical Properties of YAG and Nd:YAG Single Crystals. *Mater. Research Bulletin* **2015**, *63*, 80-87.

[2] Zhang, M.; Guo, H.; Han, J.; Zhang, H.; Xu, C. Distribution of Neodymium and Properties of Nd:YAG Crystal by Horizontal Directional Solidification. *J. Cryst. Growth* **2012**, *340*, 130-134.

[3] Gruber, J. B.; Hills, M. E.; Allik, T. H.; Jayasankar, C. K.; Quagliano, J. R.; Richardson, F. S. Comparative Analysis of Nd^{3+} ($4f^3$) Energy Levels in Four Garnet Hosts. *Phys. Rev. B* **1990**, *41*, 7999-8012.

[4] Pavel, N.; Lupei, V.; Taira, T. 1.34-μm Efficient Laser Emission in Highly-Doped Nd:YAG Under 885-nm Diode Pumping. *Opt. Express* **2005**, *13*, 7948–7953.

[5] Kaminskii, A. A. Laser Crystals. *Springer* **1981**.

[6] Deserno, U.; Ross, D.; Zeidler, G. Quasicontinuous Giant Pilse Emission of $^4F_{3/2} \rightarrow {}^4I_{13/2}$ Transitions at 1.32 μm in YAG:Nd^{3+}. *Phys. Lett.* **1968**, *28A*, 422-423.

[7] Krupke, W. F. Radiative Transition Probabilities Within the $4f^3$ Ground Configuration of Nd:YAG. *IEEE J. Quantum Electron.* **1971**, *7*, 153-159.

[8] Lupei, V.; Pavel, N.; Taira, T. Laser Emission in Highly Doped Nd:YAG Crystals Under $^4F_{5/2}$ and $^4F_{3/2}$ Pumping. *Opt. Lett.* **2001**, *26*, 1678-1680.

[9] Kramer, M. A.; Boyd, R. W. Three-Photon Absorption in Nd-Doped Yttrium Aluminum Garnet. *Phys. Rev. B* **1981**, *23*, 986-991.

[10] Gorller-Walrand, C.; Binnemans, K. Handbook on the Physics and Chemistry of Rare Earths, ed. Gschneidner, K. A. and Eyring, L. *Elsevier Science* **1996**, *23*.

[11] Henderson, B.; Imbusch, G. F. Optical Spectroscopy of Inorganic Solids. *Clarendon Press, Oxford* **1989**.

[12] Yeung, Y. Y.; Newman, D. J. High Order Crystal Field Invariants and the Determination of Lanthanide Crystal Field Parameters. *J. Chem. Phys.* **1986**, *84*, 4470-4473.

[13] Walrand, C. G.; Fluyt, L.; Ceulemans, A.; Carnall, W. T. Magnetic Dipole Transitions as Standards for Judd-Ofelt Parametrization in Lanthanide Spectra. *J. Chem. Phys.* **1991**, *95*, 3099–3106.

[14] Hehlen, M. P.; Brik, M. G.; Krämer, K. W. 50th Anniversary of the Judd-Ofelt Theory: An Experimentalist's View of the Formalism and Its Application. *J. Lumin.* **2013**, *136*, 221–239.